JACS
JOURNAL OF THE AMERICAN CHEMICAL SOCIETY
Cite This: J. Am. Chem. Soc. 2018, 140, 2397−2400
Communication
pubs.acs.org/JACS

Suppressing Ion Transfer Enables Versatile Measurements of Electrochemical Surface Area for Intrinsic Activity Comparisons

Youngmin Yoon, Bing Yan, and Yogesh Surendranath*

Department of Chemistry, Massachusetts Institute of Technology, Cambridge, Massachusetts 02139, United States

Supporting Information

ABSTRACT: Correlating the current/voltage response of an electrode to the intrinsic properties of the active material requires knowledge of the electrochemically active surface area (ECSA), a parameter that is often unknown and overlooked, particularly for highly nanostructured electrodes. Here we demonstrate the power of nonaqueous electrochemical double layer capacitance (DLC) to provide reasonable estimates of the ECSA across 17 diverse materials spanning metals, conductive oxides, and chalcogenides. Whereas data recorded in aqueous electrolytes generate a wide range of areal specific capacitance values (7−63 μF/real cm^2), nearly all materials examined display an areal specific capacitance of 11 ± 5 μF/real cm^2 when measured in weakly coordinating KPF_6/MeCN electrolytes. By minimizing ion transfer reactions that convolute accurate DLC measurements, we establish a robust methodology for quantifying ECSA, enabling more accurate structure-function correlations.

Conductive electrodes are central to a wide variety of devices including batteries, fuel cells, electrolyzers, capacitors, and sensors. In each case, the performance of the electrode is a summation of the intrinsic properties of the electroactive material and a key extrinsic factor, the surface area of the electrode. Thus, a careful account of the electrochemically active surface area (ECSA) is essential for correlating the aggregate performance of an electrode to the intrinsic properties of the material under investigation. This is particularly true for highly nanostructured electrodes, for which dramatic variations in ECSA between different electrode preparations[1,2] can obscure the underlying intrinsic performance metrics that are required for accurate structure-function correlations, comparisons to theoretical models, and rational materials design.

Numerous complementary methods exist for measuring ECSA, but with significant limitations. Gas adsorption analysis typically requires a minimum surface area of ∼1000 cm^2, far greater than the 0.1−100 cm^2 values typical of common laboratory scale electrodes.[3] This sensitivity challenge can be overcome using electrochemical adsorption probes such as underpotential deposition (UPD), CO stripping, and surface monolayer oxidation.[4,5] Unfortunately, since these probes rely on chemisorption, they can only be applied to a limited subset of surface structures (e.g., appropriate facets of noble metals) that display the necessary adsorption thermochemistry and kinetics. Additionally, these adsorption methods often utilize acutely toxic chemical probes including Tl, Cd, Pb, Hg, and CO, that impede routine use.[4−6] Moreover, these methods often destroy the surface by inducing restructuring and/or irreversible alloying that prevents repeated measurements of the same electrode.[7−9] Electrochemical adsorption probes are also prone to error stemming from the nonsystematic integration of surface waves that are convoluted by adjacent bulk redox features and variable capacitive baselines.[4,5,10] Clearly, more general electrochemical methods for measuring ECSA across diverse materials are desired.

For the vast majority of materials for which well-characterized adsorption probes are not available, double layer capacitance (DLC) measurements offer a versatile and nondestructive alternative for estimating ECSA. The DLC reports directly on the amount of charge accumulated at the electrode surface, and is thus directly correlated to the ECSA.[2,5,10,11] Therefore, DLC measurements could be used as a general tool for estimating ECSA across diverse materials provided that each material displays a similar capacitance per real surface area (specific capacitance). Unfortunately, ion transfer reactions at the interface, including corrosion, intercalation, and specific adsorption, can lead to additional current that convolutes the DLC measurement, introducing large variability in specific capacitance values[5,10−12] across materials. These convoluting reactions are particularly pronounced for metal oxide and chalcogenide surfaces, for which H^+/OH^- adsorption can inflate specific capacitance values by as much as an order of magnitude.[11] Given the central role of surface proton transfer in these chemisorption processes, we postulated that DLC data collected in polar aprotic electrolytes would permit the observation of more uniform specific capacitance values across diverse materials (Figure 1).

Herein, we use atomic force microscopy (AFM) surface area measurements to calculate specific capacitance values across 19 materials spanning metals, metal oxides, and metal chalcogenides. Using these data, we establish simple DLC measurement protocols in CH_3CN electrolytes, which are readily prepared with low water content, display high conductivity, and are relatively chemically inert. We find that diverse materials exhibit similar specific capacitance values in this aprotic electrolyte, establishing a powerful empirical methodology for estimating ECSA, thereby allowing for systematic comparisons of intrinsic electrode activity.

To quantify specific capacitance values (measured in μF/real cm^2) across various materials and measurement conditions, we measured the real surface area of each electrode using AFM, an

Received: October 13, 2017
Published: December 21, 2017

DOI: 10.1021/jacs.7b10966
J. Am. Chem. Soc. 2018, 140, 2397−2400

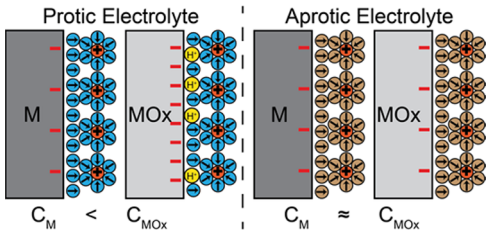

Figure 1. Comparison of capacitive electrode response for metals (C_M) and oxides (C_{MOx}). H^+ adsorption in protic electrolytes (left, blue) leads to higher capacitance for oxides (C_{MOx}) than for metals (C_M). This work postulates similar capacitance for disparate materials in a weakly adsorbing aprotic electrolyte (right, brown).

established method for determining the surface areas of nominally planar thin film electrodes.[5,10,13] AFM measurements are independent of the surface chemistry of the material but are limited to characterizing nonporous substrates. Thus, we synthesized dense thin film electrodes of various compositions using metal evaporation techniques and electrodeposition. Using these methods, we examined 19 planar, nonporous, thin-film electrodes spanning noble metals (Ag, Au, Pd, Pt), oxide-passivated base metals (Al, Cr, Fe, Mo, Ni, $Ni_{0.8}Fe_{0.2}$, Ta, Ti), conductive carbon (graphite), bulk conductive oxides (F-doped SnO (FTO), $NiFeO_x$, RuO_2), and metal chalcogenides ($CoSe_x$, $NiSe_x$, NiS_x). In all cases, AFM measurements revealed highly planar films with roughness factors of 1.0−1.1 (see SI for AFM height profiles for all materials). The AFM-derived roughness of each electrode was then used to calculate the surface area of each sample and its specific capacitance.

To investigate the impact of protic electrolytes on DLC measurements, we compared specific capacitance values recorded in 0.15 M $NaClO_4$ aqueous electrolyte with those measured in 0.15 M KPF_6 with CH_3CN electrolyte. In all cases, DLC measurements were performed by recording cyclic voltammetry (CV) cycles over a narrow range (±50 mV) centered around the open circuit potential (OCP). CV cycling was repeated using a range of scan rates from 5 to 50 mV/s. The capacitive current at the OCP was plotted vs scan rate, and the DLC values were extracted from slopes of these plots (Figure S1, see Supporting Information (SI) for details). DLC values were then divided by the AFM-derived surface area of each electrode to determine the specific capacitance of the material under investigation.

Specific capacitance values measured in aqueous media display a wide variability across the materials explored, despite precautions taken to minimize specific adsorption of electrolyte ions. All aqueous DLC data were recorded in 0.15 M $NaClO_4$ (Figure 2), and this electrolyte was chosen because both the Na^+ cation and the ClO_4^- anions are known to be well-hydrated and weakly coordinating to metal surfaces.[14,15] Under these conditions, noble metals such as Au and Pd display specific capacitance values of ~8 $\mu F/cm^2$, at the low end of the values typically assumed for a metal surface.[16−18] This suggests that for these materials, DLC measurements are not dramatically convoluted by specific adsorption contributions and accurately reflect the true surface areas of the materials. Ag and Pt display larger specific capacitance values of 40 and 35 $\mu F/cm^2$ in aqueous electrolyte, perhaps due to the impact of strongly adsorbed OH_x species at the OCP values of 0.8 and 0.85 V vs the reversible hydrogen electrode (RHE), respectively. In contrast, metallic electrodes with oxidic surface chemistry exhibit specific capacitance values 2−6 times greater than that of these noble

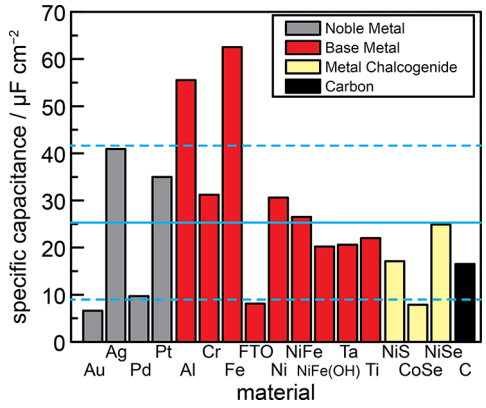

Figure 2. Comparison of specific capacitance values of noble metals (gray), surface oxide passivated base metals (red), metal chalcogenides (yellow), and carbon (black) measured by double layer capacitance at ±50 mV of the open circuit potential in 0.15 M $NaClO_4$ aqueous electrolyte. The solid and dotted blue lines denote the average and standard deviations of the specific capacitance values across the tested materials.

metal surfaces. This increase has been well documented and is attributed, in part, to H^+/OH^- adsorption at the amphoteric oxide surface.[8,17] Interestingly, FTO electrodes display an 8-fold lower specific capacitance than oxide-terminated Fe electrodes, highlighting the extreme sensitivity of these adsorption processes on surface composition and structure. Likewise, metal chalcogenides display specific capacitance values that vary by a factor of 3 between Ni and Co. In aggregate, across 17 of the 19 materials explored (see below for a detailed discussion of MoO_x and RuO_2 outlier materials), we observe an average specific capacitance of 26 $\mu F/cm^2$ with a large standard deviation of ±16 $\mu F/cm^2$ and a total range of 7−63 $\mu F/cm^2$. Together, these data suggest that aqueous electrolytes are prone to a large variability in specific DLC across materials due to a diversity of surface adsorption equilibria.

DLC data collected in polar, aprotic CH_3CN media display significantly less variability (Figure 3). Nonaqueous specific capacitance values were recorded in CH_3CN electrolyte

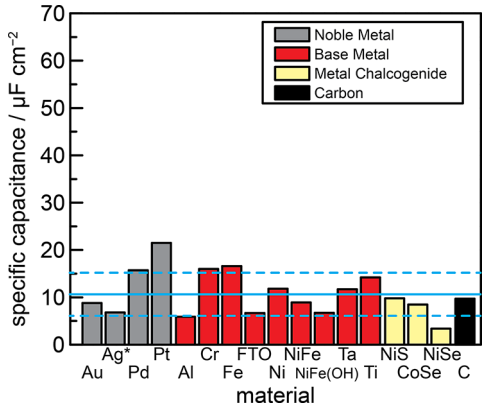

Figure 3. Comparison of specific capacitance values of noble metals (gray), surface oxide passivated base metals (red), metal chalcogenides (yellow), and carbon (black) measured by double layer capacitance at ±50 mV of the open circuit potential in 0.15 M KPF_6, CH_3CN electrolyte. The solid and dotted blue lines denote the average and standard deviations of the specific capacitance values across the tested materials. *Ag was measured at −600 mV vs the reference due to corrosion at the OCP.

DOI: 10.1021/jacs.7b10966
J. Am. Chem. Soc. 2018, 140, 2397−2400

containing 0.15 M KPF_6, using the protocol described above. In contrast to the DLC values in H_2O, specific capacitance values in CH_3CN display a range of 3.4−17 $\mu F/cm^2$, with an average of 11 and a standard deviation of 4.7. Whereas metal electrodes display a slight rise in capacitance relative to measurements in water, most metal oxides display a significantly lower capacitance. For example, oxide passivated Al and Fe electrodes display values of 6 and 17 $\mu F/cm^2$ in CH_3CN electrolyte, respectively, compared to 56 and 63 $\mu F/cm^2$ in water. Included in the group of oxides is $NiFeO_x$, a potent catalyst for oxygen evolution, which shows a specific capacitance of 6.7 $\mu F/cm^2$, close to the mean value of 11 $\mu F/cm^2$.[20,21] Although we expect this method will underreport the internal surface area between the layers of this oxide due to inhibited ion intercalation, these data suggest that nonaqueous DLC may be a viable method for comparing the bulk-solvent-exposed ECSA of oxidic OER catalysts. Likewise, the nonaqueous DLC values of metal chalcogenides fall relative to their aqueous values and, apart from NiSe, exist within one standard deviation of the mean value. Together, the data suggest that, remarkably, apart from the MoO_x and RuO_2 outliers discussed below, aprotic CH_3CN DLC values will generate a reasonable estimate of ECSA (within a factor of ~1.8) across diverse materials classes by applying the assumption of a common, empirical specific capacitance value of 11 $\mu F/cm^2$. This empirical value is reasonable considering the solvated radii of K^+, PF_6^-, and the dielectric properties of the interface (see SI).[18] Given that the electrochemical and, in particular, electrocatalytic performances of various materials typically differ by orders of magnitude, this level of precision, while imperfect, is well suited to benchmarking performance across diverse high surface area materials which are not amenable to traditional adsorption probes of ECSA.[2,11] Additionally, AFM roughnesses for Au and Ti electrodes were unchanged following DLC measurements under aprotic conditions (Table S1), suggesting that the technique preserves the native surface area of the electrode.

Even in the limit where specific adsorption is negligible, the structure of the electrolyte ions impacts the accuracy of the DLC measurement. To best approximate the ECSA, a rectangular CV scan with a broad current plateau across the potential range is ideal, as it maximizes the linearity in the DLC plot of capacitance current vs scan rate. As highlighted in Figure 4 for oxide-passivated Ti electrodes, this ideal limiting behavior is highly sensitive to the structure of the electrolyte ions. Whereas KPF_6 electrolytes give rise to broad plateaus, CV scans recorded in bulkier tetrabutylammonium hexafluorophosphate (TBA-PF_6) electrolytes display noticeable curvature, indicative of sluggish ion rearrangement. While series resistance can contribute to sloping, this has a negligible contribution for these conductive electrodes polarized in a concentrated electrolyte medium. Indeed, the degree of curvature increases with increasing scan rate, reflecting the slower kinetics of rearranging bulkier TBA^+ relative to K^+ ions.[22,23] Sluggish electrolyte rearrangement contributes to greater nonlinearity in the plots of DLC vs scan rate (Figure S3). While this nonlinearity contributes to a relatively small change in capacitance (13.0 vs 12.7 μF) for this planar TiO_x example, the error will be more pronounced for micro-/mesoporous materials that exhibit impeded ion transport. For these high surface area materials, capacitance data collected at very low scan rates are likely to be most reflective of the true surface area. We stress that for some materials (see below) electrolyte ion intercalation can significantly convolute DLC data and, in these cases, larger ions may be unavoidable. Nonetheless, the data indicate that, for most materials, smaller

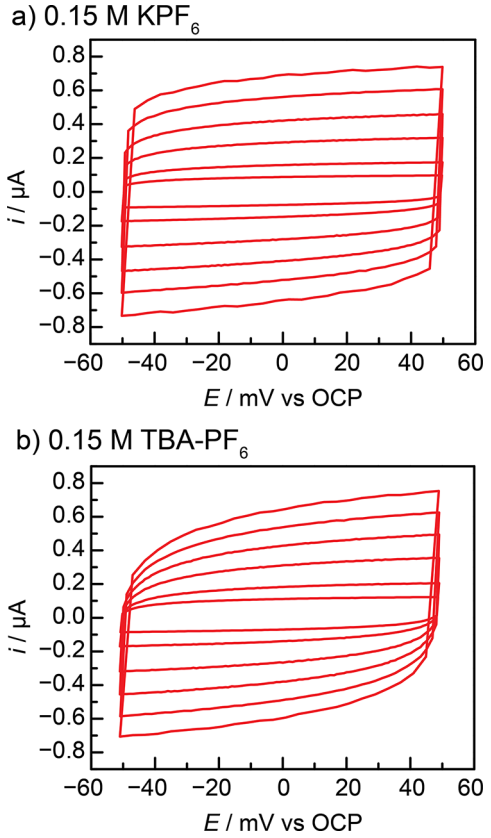

Figure 4. CV scans near the open circuit potential (OCP) for the same oxide-passivated Ti electrode in CH_3CN with 0.15 M (a) KPF_6 and (b) TBA-PF_6.

electrolyte ions are essential for maximizing the rate of interfacial ion rearrangement, a prerequisite for accurate DLC measurements.

Unlike ion size, the concentration of the electrolyte has minimal impact on the DLC measurement (Figure S4). For Au electrodes, very similar specific capacitance values of 8.4 ± 0.4 $\mu F/cm^2$ were obtained over a range of electrolyte concentrations from 0.05 to 0.15 M KPF_6, indicating a minimal dependence on electrolyte strength over this range. Similarly, oxide-passivated Ni electrodes display specific capacitance values of 12.7 ± 0.6 $\mu F/cm^2$ over the same range of electrolyte concentrations. While classical double layer theory predicts a strong dependence of the capacitance on electrolyte strength near the potential of zero charge (PZC), our data suggest that this effect is minimal for the samples investigated here. Indeed, PZC values are typically facet dependent and the polycrystalline nature of the samples explored here may impede clear observation of this phenomenon.[17] Furthermore, capacitance minima near the PZC are typically not observed for the relatively high electrolyte strengths examined here.[17] We stress that high electrolyte concentrations are typically preferred for DLC measurements to ensure high solution conductivity and a high ion concentration at the double layer. In this limit, further variations in electrolyte strength do not dramatically alter the measured capacitance.

The foregoing data indicate that DLC measurements in KPF_6/CH_3CN electrolytes provide good estimates of ECSA across diverse materials. However, the proposed approach is not well suited to all materials. In particular, known supercapacitor materials such as RuO_2 and oxide-passivated Mo (MoO_x) still display significant ion transfer currents in KPF_6/CH_3CN

DOI: 10.1021/jacs.7b10966
J. Am. Chem. Soc. 2018, 140, 2397−2400

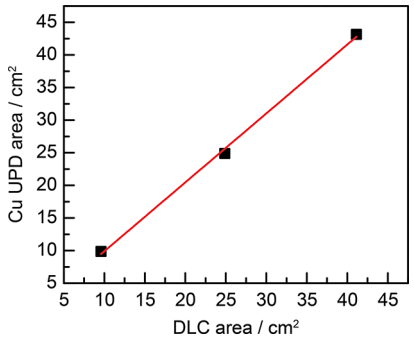

Figure 5. ESCA measured by Cu UPD vs ECSA measured by DLC for high surface area electrodeposited Au.

electrolytes, making them unsuitable for DLC-ECSA analyses using the procedure presented in this work (Figure S5). Planar RuO_2 and oxide-passivated Mo display elevated specific capacitance values of 125 and 297 $\mu F/cm^2$ in H_2O at the OCP, respectively, reflecting the high degree of proton and ion adsorption/intercalation in these supercapacitor materials. In aprotic CH_3CN/KPF_6 electrolyte, RuO_2 and MoO_x exhibit decreased yet large specific capacitance values of 107 and 29 $\mu F/cm^2$. These high values may arise from specific adsorption/intercalation of electrolyte ions or interactions with trace H_2O known to exist in CH_3CN (~5 ppm).[24] Evidence for cation adsorption/intercalation appears from the fact that the specific capacitances decrease to 53 and 24 $\mu F/cm^2$ for RuO_2 and oxide-passivated Mo in the presence of bulkier TBA-PF_6 electrolyte. These studies highlight that, for new materials in particular, DLC measurements collected across a range of nonaqueous electrolytes provide the best indication of the true ECSA.

With the above caveats in mind, we examined whether nonaqueous DLC measurements could be used to estimate the surface area of highly nanostructured electrodes. We synthesized a series of high surface area Au electrodes via rapid electrodeposition[1] and measured their capacitance in 0.15 M KPF_6/CH_3CN electrolyte. Au was chosen as a model case to compare DLC-derived ECSA to the values generated using a known Cu UPD probe (Figure S6). The Cu UPD-derived ECSA values agree well with the DLC-derived ECSA over a wide range of Au roughness factors from ~10 to ~40 (Figure 5), indicating that the proposed method for ECSA determination is well suited to analyzing high surface area materials.

Through careful selection of an electrolyte that minimizes interfacial ion transfer reactions while maximizing the kinetics of electrolyte rearrangement, we have demonstrated that aprotic DLC measurements in CH_3CN yield similar (~11 $\mu F/cm^2$) specific capacitance values for a wide range of noble metals, oxide-passivated base metals, graphitic carbon, bulk conductive oxides, and metal chalcogenides. Given that the vast majority of known and emerging electroactive materials do not yield to traditional ECSA measurements, the strategy established and validated here provides a simple and powerful tool for translating the current/voltage parameters of nanostructured electrodes into intrinsic materials performance metrics that will enable systematic comparisons and guide rational materials design.

■ ASSOCIATED CONTENT

Supporting Information

The Supporting Information is available free of charge on the ACS Publications website at DOI: 10.1021/jacs.7b10966.

Full experimental details, AFM, XPS, and SEM characterization (PDF)

■ AUTHOR INFORMATION

Corresponding Author

*yogi@mit.edu

ORCID

Yogesh Surendranath: 0000-0003-1016-3420

Notes

The authors declare no competing financial interest.

■ ACKNOWLEDGMENTS

We thank A. Shoji Hall and Kurt Broderick for helpful discussions. This research was supported by the NSF under award CHE-1454060. AFM investigations made use of Shared Experimental Facilities supported in part by the MRSEC Program of the National Science Foundation under award DMR-1419807. Y.S. acknowledges the Sloan Foundation and the Research Corporation for Science Advancement (Cottrell Award).

■ REFERENCES

(1) Liu, M.; Pang, Y.; Zhang, B.; De Luna, P.; Voznyy, O.; et al. *Nature* **2016**, *537*, 382.
(2) McCrory, C. C. L.; Jung, S.; Ferrer, I. M.; Chatman, S. M.; Peters, J. C.; Jaramillo, T. F. *J. Am. Chem. Soc.* **2015**, *137*, 4347.
(3) Sing, K. S. W. *Pure Appl. Chem.* **1985**, *57*, 603.
(4) Herrero, E.; Buller, L. J.; Abruña, H. D. *Chem. Rev.* **2001**, *101*, 1897.
(5) Łukaszewski, M. *Int. J. Electrochem. Sci.* **2016**, *11*, 4442.
(6) Binninger, T.; Fabbri, E.; Kotz, R.; Schmidt, T. J. *J. Electrochem. Soc.* **2014**, *161*, H121.
(7) Vidu, R.; Hara, S. *J. Electroanal. Chem.* **1999**, *475*, 171.
(8) Oviedo, O. A.; Reinaudi, L.; Garcia, S.; Leiva, E. P. M. *Underpotential Deposition*; Monographs in Electrochemistry; Springer: Cham, 2016.
(9) Vaskevich, a; Rosenblum, M.; Gileadi, E. *J. Electroanal. Chem.* **1995**, *383*, 167.
(10) Trasatti, S.; Petrii, O. A. *Pure Appl. Chem.* **1991**, *63*, 711.
(11) McCrory, C. C. L.; Jung, S.; Peters, J. C.; Jaramillo, T. F. *J. Am. Chem. Soc.* **2013**, *135*, 16977.
(12) Fang, L.; Tao, Q.; Li, M.; Liao, L.; Chen, D.; Chen, Y. *Chin. J. Chem. Phys.* **2010**, *23*, 543.
(13) Lockett, V.; Horne, M.; Sedev, R.; Rodopoulos, T.; Ralston, J. *Phys. Chem. Chem. Phys.* **2010**, *12*, 12499.
(14) El Kadiri, F.; Faure, R.; Durand, R. *J. Electroanal. Chem. Interfacial Electrochem.* **1991**, *301*, 177.
(15) Li, C. W.; Kanan, M. W. *J. Am. Chem. Soc.* **2012**, *134*, 7231.
(16) *Comprehensive Treatise of Electrochemistry*; Bockris, J. O., Conway, B. E., Yeager, E., Eds.; Springer: Boston, 1980.
(17) Schmickler, W.; Santos, E. *Interfacial Electrochemistry*; Springer: Berlin/Heidelberg, 2010.
(18) Gileadi, E. *Physical Electrochemistry*; Wiley-VCH: Weinheim, 2011.
(19) De Koninck, M.; Poirier, S.; Marsan, B. *J. Electrochem. Soc.* **2006**, *153*, A2103.
(20) Trotochaud, L.; Young, S. L.; Ranney, J. K.; Boettcher, S. W. *J. Am. Chem. Soc.* **2014**, *136*, 6744.
(21) Miller, E. L. *J. Electrochem. Soc.* **1997**, *144*, 1995.
(22) Rodionova, L. S.; Filanovskii, B. K.; Petrov, M. L. *Russ. J. Gen. Chem.* **2001**, *71*, 85.
(23) Tsierkezos, N. G.; Philippopoulos, A. I. *Fluid Phase Equilib.* **2009**, *277*, 20.
(24) Warren, J. J.; Mayer, J. M. *J. Am. Chem. Soc.* **2008**, *130*, 7546.

DOI: 10.1021/jacs.7b10966
J. Am. Chem. Soc. 2018, 140, 2397−2400